ARL-TR-8378 ● JUNE 2018

US Army Research Laboratory

Scaling a Human Body Finite Element Model with Radial Basis Function Interpolation

by P Justin McKee

NOTICES

Disclaimers

The findings in this report are not to be construed as an official Department of the Army position unless so designated by other authorized documents.

Citation of manufacturer's or trade names does not constitute an official endorsement or approval of the use thereof.

Destroy this report when it is no longer needed. Do not return it to the originator.

ARL-TR-8378 ● JUNE 2018

US Army Research Laboratory

Scaling a Human Body Finite Element Model with Radial Basis Function Interpolation

by P Justin McKee
Weapons and Materials Research Directorate, ARL

REPORT DOCUMENTATION PAGE	*Form Approved* *OMB No. 0704-0188*

1. REPORT DATE *(DD-MM-YYYY)* June 2018	**2. REPORT TYPE** Technical Report	**3. DATES COVERED (From - To)** 1 March 2017–28 February 2018

4. TITLE AND SUBTITLE Scaling a Human Body Finite Element Model with Radial Basis Function Interpolation	**5a. CONTRACT NUMBER**
	5b. GRANT NUMBER
	5c. PROGRAM ELEMENT NUMBER
6. AUTHOR(S) P Justin McKee	**5d. PROJECT NUMBER** FPSP28
	5e. TASK NUMBER
	5f. WORK UNIT NUMBER
7. PERFORMING ORGANIZATION NAME(S) AND ADDRESS(ES) US Army Research Laboratory Weapons and Materials Research Directorate ATTN: RDRL-WMP-B Aberdeen Proving Ground, MD 21005	**8. PERFORMING ORGANIZATION REPORT NUMBER** ARL-TR-8378
9. SPONSORING/MONITORING AGENCY NAME(S) AND ADDRESS(ES)	**10. SPONSOR/MONITOR'S ACRONYM(S)**
	11. SPONSOR/MONITOR'S REPORT NUMBER(S)

12. DISTRIBUTION/AVAILABILITY STATEMENT
Approved for public release; distribution is unlimited.

13. SUPPLEMENTARY NOTES

14. ABSTRACT
Human body models are currently used to evaluate the body's response to a variety of threats to the Soldier. The ability to adjust the size of human body models is currently limited because of the complex shape changes that are required. Here, a radial basis function interpolation method is used to morph the shape on an existing finite element mesh. Tools are developed and integrated into the Blender computer graphics software to assist with defining the morph. These tools allow an existing human body model to be scaled to better capture the full range of variability that exists in the human population. The ability to better represent human variability will allow for improved comparison to validation experiments and additional insight into the effect of body shape to specific threats.

15. SUBJECT TERMS
radial basis function, model scaling, human body model, finite element, meshing

16. SECURITY CLASSIFICATION OF:			**17. LIMITATION OF ABSTRACT**	**18. NUMBER OF PAGES**	**19a. NAME OF RESPONSIBLE PERSON** P Justin McKee
a. REPORT Unclassified	**b. ABSTRACT** Unclassified	**c. THIS PAGE** Unclassified	UU	20	**19b. TELEPHONE NUMBER (Include area code)** 410-278-3031

Standard Form 298 (Rev. 8/98)
Prescribed by ANSI Std. Z39.18

Contents

List of Figures

1. Introduction

Development of a human body finite element (FE) model presents many unique challenges. A particular challenge is the complex geometry that makes creation and modification of an FE mesh difficult and time consuming. In many cases, a human body FE model is developed to represent a 50th percentile human by height and weight. However, there is a large amount of variability in human size and shape. The ability to adjust an existing FE model will allow for better comparison to validation experiments, a better assessment of a threat to a variable population, and a reduction in time spent developing the mesh.

The human body has a complex shape made of many components. A simple global scaling will not capture the changes in size and shape that are necessary to accurately represent the human population. Therefore, it is necessary for a scaling tool to apply scaling that is relevant for each specific component of the body. Here, a radial basis function (RBF) interpolation method is applied to a mesh of the human torso as well as individual components of the body. This approach has previously been used to create interpolated surfaces from medical images,[1] warp medical images,[2] and morph FE meshes,[3,4] including the human body at the component,[5] system,[6] and full body levels.[7–9] The RBF method allows for a change in shape to be defined by reference points in an initial mesh along with their updated positions in the new shape. The volume mesh is then transformed based on coefficients that are calculated from the points. This procedure allows for a complex change in shape of the original mesh.

Additionally, tools are developed to assist with applying an RBF morph to an FE mesh. The Blender computer graphics program is used to visualize the mesh and define reference and target points. Python scripts interface with Blender to obtain the coordinates of the reference and target points, which are used to calculate the coefficients that define the morph. The morph is then applied to all of the nodes of the FE mesh. The goal of this process is to create a robust method to reshape an existing mesh in a variety of complex ways. Examples are provided to show a simplified approach to scale a group of body parts as well as a more detailed method to apply an irregular shape change to a single component. Element quality statistics are provided to show that the morph is applied without a significant reduction in element quality.

2. Methods

2.1 Scaling Method

The RBF method uses a set of known vector translations and a vector field is interpolated in the space between these known points.[2] The generalized form of the interpolation is described by Carr et al.[1] In this report, the components of the 3-D interpolated translation, **s**, are defined by

$$s_1(\mathbf{x}) = \sum_{i=1}^{N} \varphi(\|\mathbf{x}-\mathbf{x}_i\|)\mathbf{W}_{i,1} + C_{1,1}x_1 + C_{2,1}x_2 + C_{3,1}x_3 + C_{4,1}, \quad (1)$$

$$s_2(\mathbf{x}) = \sum_{i=1}^{N} \varphi(\|\mathbf{x}-\mathbf{x}_i\|)\mathbf{W}_{i,2} + C_{1,2}x_1 + C_{2,2}x_2 + C_{3,2}x_3 + C_{4,2}, \quad (2)$$

$$s_3(\boldsymbol{x}) = \sum_{i=1}^{N} \varphi(\|\boldsymbol{x}-\boldsymbol{x}_i\|)\boldsymbol{W}_{i,3} + C_{1,3}x_1 + C_{2,3}x_2 + C_{3,3}x_3 + C_{4,3}. \quad (3)$$

Here, **x** is the position of a point in $\mathbb{R}^3$ with components x_1, x_2, and x_3, N is the number of points in the set of reference points, φ is a radial kernel that operates on the Euclidian distance from one point to another, **W** is an N by 3 matrix of weighting coefficients, and **C** is a 4 by 3 matrix of coefficients that must be solved for. φ can be defined as one of several possible functions. In this work, φ is defined by

$$\varphi(\mathbf{x}) = \|\mathbf{x}-\mathbf{x}_i\|^3, \quad (4)$$

as this has been shown to produce good quality mesh morphing in work by Sieger et al.[4] This interpolation function will provide a unique solution when nodes are not coplanar.[1]

First, the reference and target points are chosen for the mesh. Reference points can be placed at easily identifiable landmarks or any other location that is important and predictable when adjusting the size of the mesh. Target points are the updated coordinates of the reference points after scaling is applied. The reference and target points are used to solve for the weighting coefficients **W** and polynomial coefficients **C** using the linear system

$$\begin{bmatrix} \varphi(\|\mathbf{x}_i-\mathbf{x}_j\|) & \mathbf{P} \\ \mathbf{P}^T & \mathbf{0} \end{bmatrix} \begin{bmatrix} \mathbf{W} \\ \mathbf{C} \end{bmatrix} = \begin{bmatrix} \mathbf{T} \\ \mathbf{0} \end{bmatrix}, \quad (5)$$

where $\mathbf{x}_i$ and $\mathbf{x}_j$ are the reference points in the set from 1-N, **P** is a matrix containing the reference point positions that are used to solve for the polynomial coefficients $\mathbf{C}_{1\text{-}4}$

$$\boldsymbol{P} = \begin{bmatrix} x_{1,1} & x_{1,2} & x_{1,3} & 1 \\ \vdots & \vdots & \vdots & \vdots \\ x_{N,1} & x_{N,2} & x_{N,3} & 1 \end{bmatrix}, \quad (6)$$

and **T** is the translation from the reference points to the target points. Finally, Equation 1 can be applied to solve for the translation of all nodes in the mesh using the coefficients that were determined from the reference points.

2.2 Scaling Tools

Scripts to calculate and apply a morph have been developed using Python. The basic morphing tool makes use of text-based commands to accept user-defined reference and target point locations as well as an initial mesh. The RBF interpolation coefficients are calculated, and the resulting morph is applied to the mesh. However, complex geometry such as the human body can require many reference points to define an acceptable morph. Therefore, additional tools have been created to assist with defining reference and target points. Python scripts have been made to interface with the Blender computer graphics program (version 2.79).[10] Blender offers many capabilities to easily manipulate surface geometry compared to the difficulties of editing an FE volume mesh. Surfaces are created in Blender where the vertices will become the reference and target points used to calculate the RBF interpolation coefficients. These will be referred to as reference surfaces and target surfaces.

Two examples are presented using components of the US Army Research Laboratory (ARL) human body model, which is based on 50th percentile male geometry. The ultimate goal of the procedure is to define a set of reference vertices and a matching set of target vertices with an updated location. The scaling procedure is currently in a generalized state where the reference and target vertices must be created by the user using the tools available in Blender. The best method to do this is dependent on the specific problem. The examples presented in this report demonstrate two possible methods that can be used obtain the reference and target vertices.

The first example uses the torso model that contains the ribs, thoracic and lumbar vertebrae, clavicle, scapula, organs, homogenized flesh, and skin. The chest depth and width measured at the 4th rib interspace are reduced to 78.8% and 85.4% of their initial dimensions, respectively. The goal of this example is to show how scaling can be applied to a complex system made up of skin, bones, and organs using simple shapes that represent the topology of the body. This method is useful when attempting to scale a component of the body without detailed sizing information available. The procedure is illustrated in Fig. 1. Planes are created in Blender along the length of the torso in the body's transverse plane that will be used as the reference and target surfaces. This allows adjustments to the full model by moving a reduced number of vertices compared to editing the full surface. The first plane is created at the 4th rib interspace to match the location where the measurements of torso depth and width are made. Other planes are made at locations that can capture the shape of the body. The reference planes are shown in Fig. 1a. The vertices marked with the red dot are initially at the exterior surface of the skin. These vertices can slide along their connected edges to adjust the chest depth and width. Motion of the lateral vertices is mirrored to ensure that chest width remains symmetrical. Figure 1b shows the updated target planes with the moved vertices marked by blue dots and their original positions marked by hollow red dots. The coefficients of the RBF interpolation are found using the change in position of the vertices between the reference and target planes, and the morph is applied to the volume mesh.

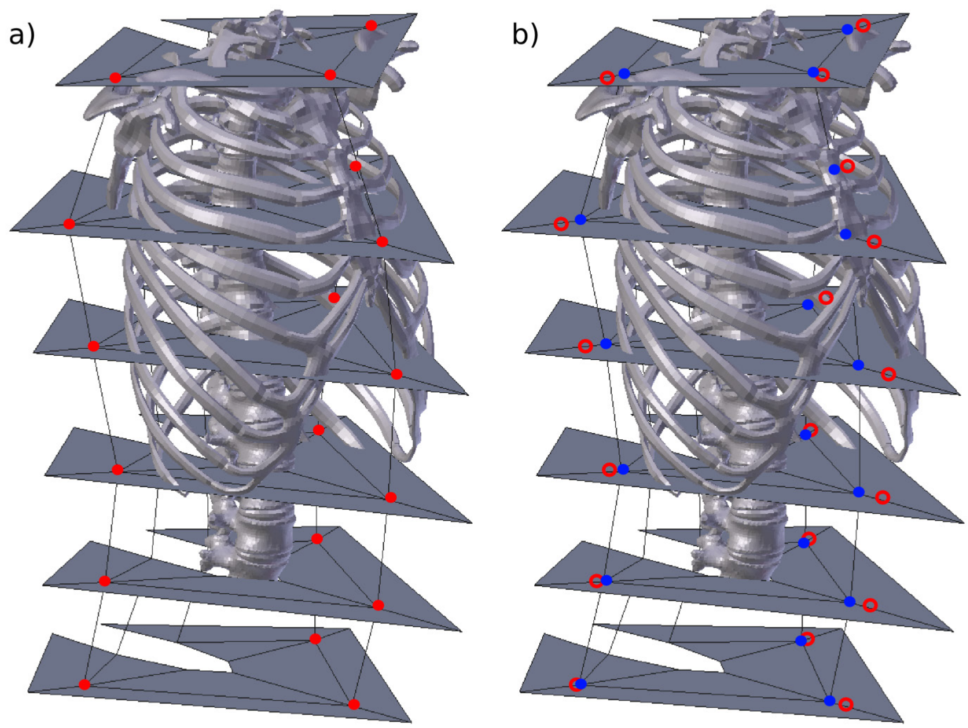

Fig. 1 The process of using simplified surfaces in Blender to define reference and target surfaces: a) vertices on the initial surfaces can slide along edges; b) vertices are moved inward to define a morph with reduced chest width and depth

The second example makes use of the full surface of the calcaneus to define a more complex target surface. The goal of this example is to show the ability to make detailed adjustments to individual components. Shell elements from the initial mesh are imported into Blender to define the reference surface. This surface is then duplicated to make a new target surface that is edited directly. This method is most useful when volume image stacks such as magnetic resonance imaging (MRI) or computed tomography (CT) provide detailed information about the target shape. The largest translation between vertices of the reference and target surface is 5.9 mm and the new volume is 8.5% larger than the original calcaneus. This is illustrated in Fig. 2 where the red surface is the imported calcaneus reference surface and the blue surface is the edited target surface. This approach allows for an irregular target surface to be easily created. However, it is limited by the number of vertices on the surface and memory required to solve for the coefficients of the RBF interpolation using the linear system. Computational costs can be reduced by simplifying the imported surface by merging surface vertices before the target surface is edited or by applying the morph based on a subset of vertices on the surface.

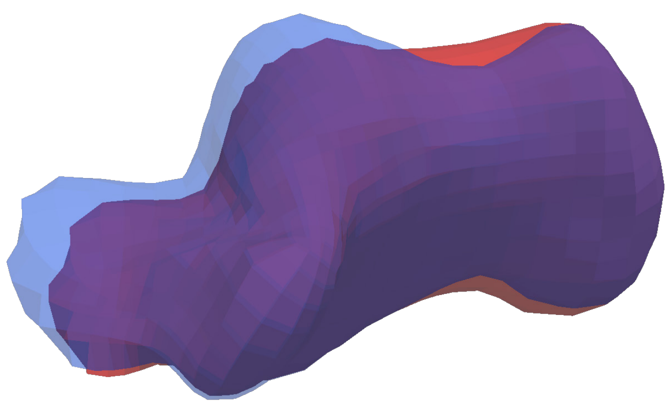

Fig. 2 The initial imported calcaneus mesh (red) is duplicated and edited to create a target surface (blue)

3. Results

A morph is considered successful if it is able to achieve the desired change in size and shape while maintaining the quality of the mesh. ANSYS ICEM CFD meshing software is used to calculate the determinant as a metric of element quality, and a histogram is shown for all example problems.

The results of the torso scaling are shown in Fig. 3. The initial torso mesh is shown in red, and the torso with reduced chest depth and width is shown in blue. This image shows that the simplified surfaces that were used to define the morph produced a smooth scaling over the length of the torso. Initial element penetration is not detected in the initial or scaled mesh. The torso initially has a minimum determinant of 0.02 with an average determinant of 0.64. After applying the morph, the minimum determinant is 0.02 with an average determinant of 0.64. Figure 4 shows a histogram of the percent of elements in each quality range that results from reducing the depth and width of the torso mesh. This plot shows that the percentage of elements in each quality range remains similar before and after the morph is applied.

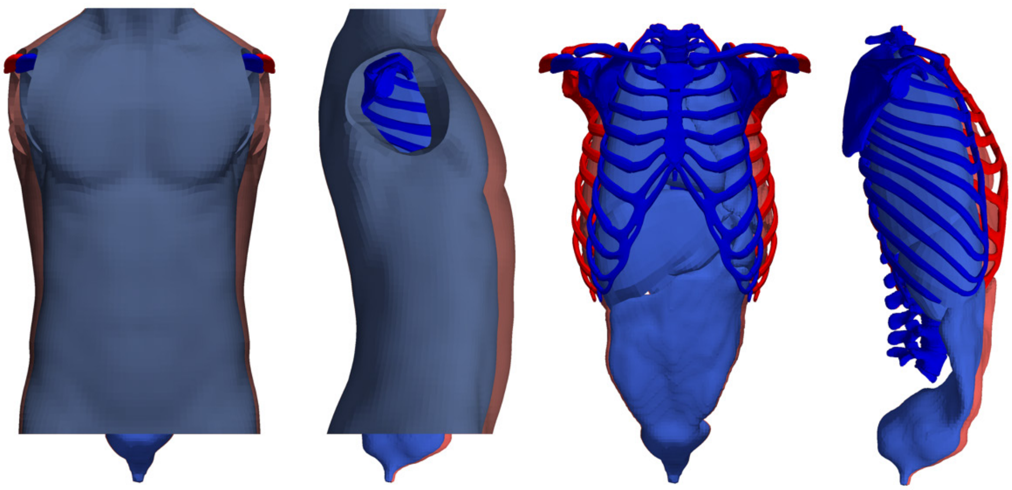

Fig. 3 Torso mesh before (red) and after (blue) the RBF interpolation is applied to reduce the chest depth and width

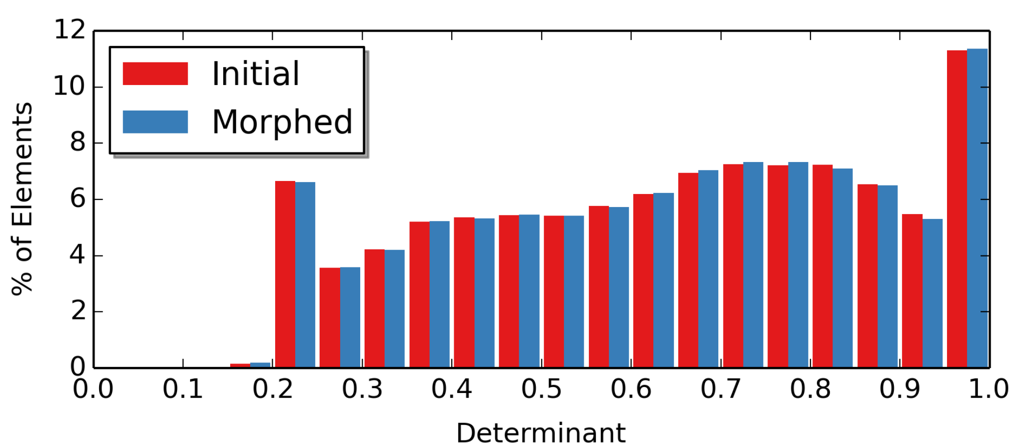

Fig. 4 Histogram of element quality between the initial torso and a torso with reduced chest width and depth

Approved for public release; distribution is unlimited.

Figure 5 shows the morphed calcaneus mesh overlaid with contour lines of the target surface. The outer surface of the calcaneus mesh matches well with the target surface because all of the surface nodes were used as reference and target points.

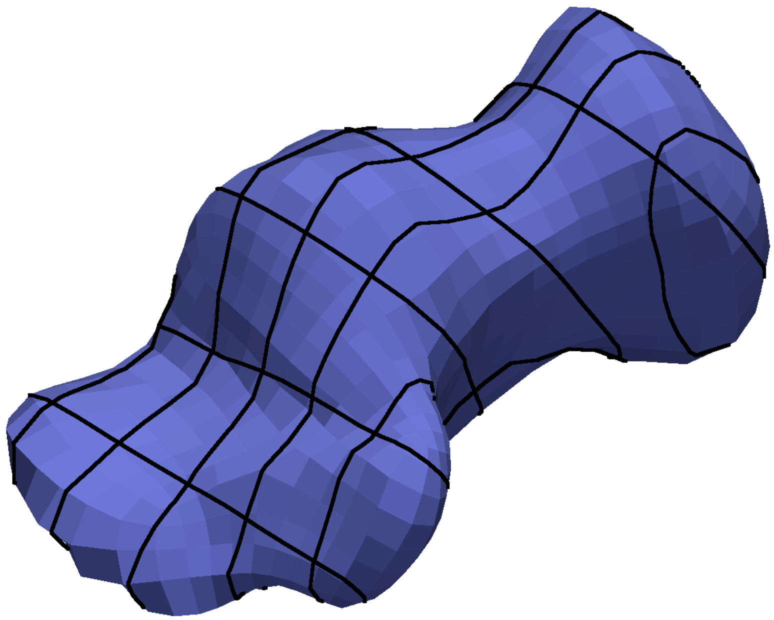

Fig. 5 Morphed calcaneus mesh overlaid with contour lines of the target surface

The calcaneus initially has a minimum determinant of 0.2 with an average determinant of 0.72. After applying the morph, the minimum determinant is 0.13 and the average determinant is 0.70. Figure 6 shows a histogram of the determinant. The percent of elements remains similar in all quality ranges except for the highest and lowest determinant ranges. There is a drop in the percentage of elements in the quality range between 0.9 and 1.0, and there are also a small number of elements where the determinant has been reduced below the initial minimum quality. An additional smoothing operation performed in ICEM CFD is able to improve the minimum determinant from 0.13 to 0.28. Smoothing the mesh improves lower-quality elements but is not able to correct the loss in quality at the higher range.

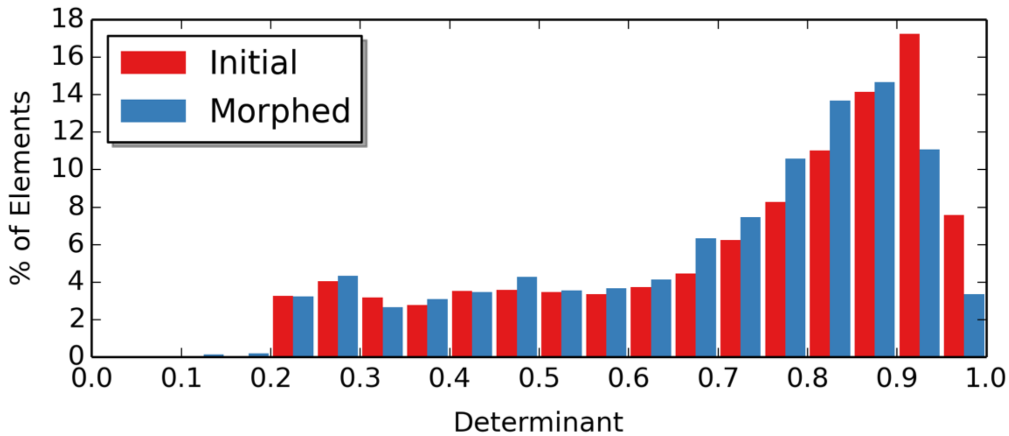

Fig. 6 Histogram of element quality between the initial and morphed calcaneus

4. Discussion

The goal of this work is to develop a means to easily apply RBF-based mesh morphing. To accomplish this goal, the procedure has been integrated into an established software to assist with defining the necessary parameters. Blender integration allows for both complex and simple scaling to be defined with a powerful graphic interface that offers many tools for moving and modifying surfaces and vertices. The examples provided here show that individual components as well as complex systems can be scaled and morphed without significant loss in element quality.

The tools that have been developed are currently in a generalized state. Examples are provided with application to the human body, but these tools can be applied to any FE mesh or faceted geometry. The generalized approach allows for flexibility in defining the morph, but also depends on the user to provide surfaces to use as input. Scaling of the human body could be streamlined based on anthropomorphic criteria. It is possible for future work to provide predefined shape changes for a variety of body types without the need to create reference and target shapes. This would simplify the use of the mesh morphing tools when applied to the human body. Also, methods to directly use medical images such as MRI or CT to define reference and target points would provide additional utility as an alternative approach.

The mesh morphing process has several limitations. Attempting to apply rotations that cause large changes in curvature to a surface can result in poor quality or inverted elements. Movement of vertices perpendicular to the reference surface normal can result in shearing of elements. This is minimized in the calcaneus example by using Blender's normal translation mode and proportional editing when creating the target surface. However, editing of a full surface is still more difficult to control compared to using a lower number of reference points. This is why the calcaneus example produced more loss in element quality compared to the torso example.

Finally, care must be taken to choose reference and target points that can prevent unwanted deformations. All reference points are weighted when applying the morph to the nodes based on the radial kernel of the RBF. Stationary target vertices where the reference position is the same as the target position can be used at boundaries to minimize unwanted deformation. The accuracy of this procedure is based on the number of vertices that are used. As an example, the skull mesh is included in the previous torso scaling example. A box is created around the head and used to define a grid of 184 stationary vertices within the box to prevent deformation of the skull. The largest error that results from this is 0.25 mm. Parts of the mesh can also be specified in the script to be ignored when applying the interpolated translation to fully prevent deformation. However, this can result in overlapping elements at boundaries and should also be used with care.

Other limitations of the process are the time and memory required to calculate the morph coefficients, which are based on the number or reference points. Figure 7a shows the time required to solve the linear system to find the morph coefficients when run on an Intel Xeon E5-2620 processor at 2.4 GHz relative to the number of reference points used. Figure 7b shows the memory requirement relative to the number of reference points. In both plots the markers are measured values, and the dashed line is a projected curve from a power law line fit. The calcaneus example shown here makes use of all of the surface vertices. This full surface-based scaling approach is prohibitively expensive with larger components that contain more nodes. In this case, it would be necessary to select a limited number of vertices from the surface to be used as reference and target points. An example of scaling applied to the calcaneus using a simplified representation of the surface rather than the full set of surface vertices is shown in Fig. 8. Panels a and b are the initial calcaneus surface and simplified reference surface, respectively. Panels c and d are the detailed target calcaneus from the original example and the new simplified target surface, respectively. The vertices are created on landmarks on the calcaneus in order to optimize the process to give reasonably detailed results with a minimal number of vertices. Panel e shows the resulting mesh overlaid with contour lines of the original target surface. In this example, the simplified calcaneus surface has 20 vertices compared to 834 vertices on the original surface. The mesh that results from using the simplified target surface does not exactly match the ideal target but provides a reasonable scaling and similar element quality distribution using a limited number of vertices.

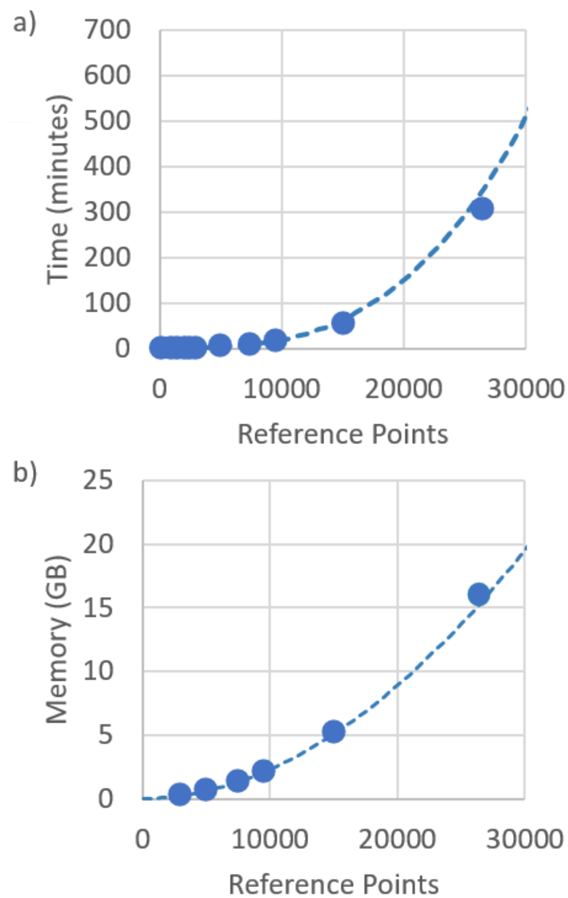

Fig. 7 a) Time and b) memory requirements to perform an RBF morph based on the number of reference points. Both requirements increase relative to the number of reference points based on a power law.

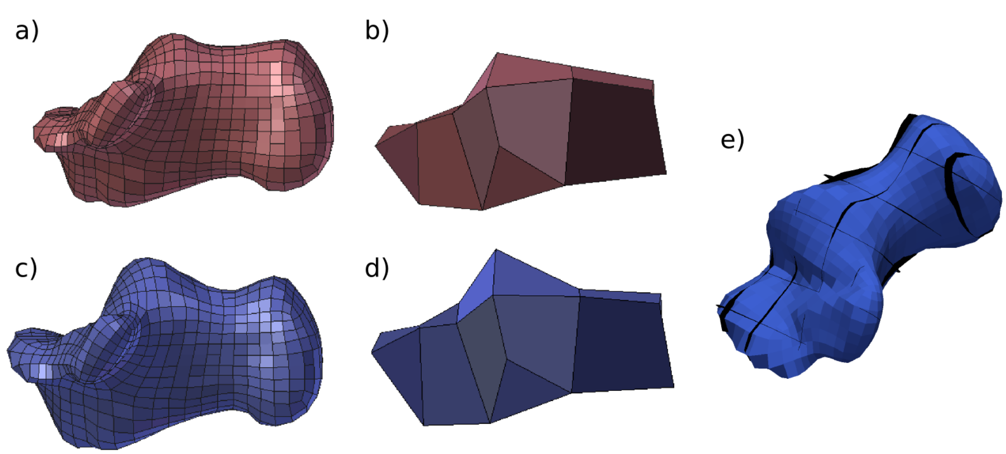

Fig. 8 a) Initial calcaneus surface, b) simplified reference surface, c) detailed target surface, d) simplified target surface, and e) resulting mesh overlaid with contour lines of the detailed target surface

5. Conclusion

This report demonstrates the use of RBF interpolation to apply a morph to an FE mesh. Tools using the Blender software have been developed to more easily define the parameters used to calculate the coefficients of the RBF interpolation. This procedure has many applications in modeling the human body. Models can be adjusted to better match the geometry of experiments for validation. The ability to change the size of a model also allows for parametric studies to investigate how body shape influences the response under various loading conditions.

6. References

1. Carr J, Fright W, Beatson R. Surface interpolation with radial basis functions for medical imaging. IEEE Trans Med Imaging. 1997;16(1):96–107.

2. Bennink H, Korbeeck J, Janssen B, ter Haar Romeny B. Warping a neuro-anatomy atlas on 3D MRI data with radial basis functions. In International Conference on Biomedical Engineering; 2006 Dec 11–14; Kuala Lampur, Malaysia.

3. De Boer A, Van der Schoot M, Bijl H. Mesh deformation based on radial basis function interpolation. Comput Struct. 2007;85(11–14):784–795.

4. Sieger D, Menzel S, Botsch M. High quality mesh morphing using triharmonic radial basis functions. Proceedings of the 21st International Meshing Roundtable; 2012 Oct 7–10; San Jose, CA.

5. Grassi L, Hraiech N, Schileo E, Ansaloni M, Rochette M, Viceconti M. Evaluation of the generality and accuracy of a new mesh morphing procedure for the human femur. Med Eng Phys. 2011;33(1):112–120.

6. Li Z, Hu J, Reed P, Rupp D, Hoff N, Zhang, J, Cheng B. Development, validation, and application of a parametric pediatric head finite element model for impact simulations. Ann Biomed Eng. 2011;39(12):2984–2997.

7. Zhang K, Cao L, Fanta A, Reed MP, Neal M, Wang JT, Hu J. An automated method to morph finite element whole-body human models with a wide range of stature and body shape for both men and women. J Biomech. 2017;60:253–260.

8. Hu J, Zhang K, Fanta A, Hwang E, Reed M. Effects of Male Stature and Body Shape on Thoracic Impact Response Using Parametric Finite Element Human Modeling. In 25th International Technical Conference on the Enhanced Safety of Vehicles (ESV) National Highway Traffic Safety Administration. 2017 Jun 5–8; Detroit, MI.

9. Hwang E, Hu J, Chen C, Klein K, Miller C, Reed M, Rupp J, Hallman J. Development, evaluation, and sensitivity analysis of parametric finite element whole-body human models in side impacts. Stapp Car Crash J. 2016;60:473–508.

10. Blender. [accessed on 2018 May 2]. https://www.blender.org.

List of Symbols, Abbreviations, and Acronyms

ARL	US Army Research Laboratory
CFD	computational fluid dynamics
CT	computed tomography
FE	finite element
MRI	magnetic resonance imaging
RBF	radial basis function

1 (PDF) DEFENSE TECHNICAL
INFORMATION CTR
DTIC OCA

2 (PDF) DIR ARL
IMAL HRA
RECORDS MGMT
RDRL DCL
TECH LIB

1 (PDF) GOVT PRINTG OFC
A MALHOTRA

39 (PDF) DIR ARL
RDRL SLB W
J GURGANUS
W MERMAGEN
RDRL WM
S SCHOENFELD
RDRL WMM A
T BOGETTI
T PLAISTED
E WETZEL
RDRL WMM B
B LOVE
P MOY
RDRL WMP B
S ALEXANDER
T BAUMER
A DAGRO
A DILEONARDI
A EIDSMORE
B FAGAN
M GRAHAM
A GUNNARSSON
C HAMPTON
C HOPPEL
M KLEINBERGER
E MATHEIS
J MCDONALD
P MCKEE
K RAFAELS
K THOMPSON
C WEAVER
T WEERASOORIYA
S WOZNIAK
T ZHANG
RDRL WMP C
R BECKER
S SATAPATHY
A SOKOLOW
RDRL WMP D
R DONEY
C RANDOW
RDRL WMP E
M BURKINS
P GILLICH
M LOVE
P SWOBODA
RDRL WMP F
N GNIAZDOWSKI
R GUPTA